

On the properties of surface reconstructed silicon nanowires

R. Ruralix and N. Lorente

Laboratoire Collisions, Agrégats, Réactivité, IRSAMC, Université Paul Sabatier,
118 route de Narbonne, 31062 Toulouse cedex, France

Abstract.

We study by means of density-functional calculations the role of lateral surface reconstructions in determining the electrical properties of $\langle 100 \rangle$ silicon nanowires. The different lateral reconstructions are explored by relaxing all the nanowires with crystalline bulk silicon structure and all possible ideal facets that correspond to an average diameter of 1.5 nm. We show that the reconstruction induces the formation of ubiquitous surface states that turn the wires into semimetallic or metallic.

1. Introduction

There has been a growing interest in semiconductor nanowires [1, 2, 3] for their potential use in future nanoelectronic applications, such as nanocontacts and nanoswitches. Silicon nanowires (SiNWs) are especially attractive for their possible efficient integration in conventional Si-based microelectronics. The use of SiNWs as chemical sensors has also been demonstrated. SiNW-based sensors for the detection of NH_3 [4], of biological macromolecules [5] and for the identification of complementary vs. mismatched DNA [6] have been reported. Experimentally, SiNWs are grown from a nanocrystal [2, 7] which is used as a seed to direct the one-dimensional crystallisation of silicon. The (typically gold) nanocluster serves as the critical point for nucleation and enables the addition of reactants that allow the growth, determining the nanowire diameter and orientation. Ma et al. [8] achieved the thinnest SiNWs reported so far, with diameters as small as 1.3 nm for a wire grown along the $\langle 110 \rangle$ direction. A few other groups [7, 9, 10] also obtained SiNWs with diameters below 10 nm and growth orientations including $\langle 100 \rangle$ [7], $\langle 110 \rangle$ [7, 9], $\langle 111 \rangle$ [9] and $\langle 112 \rangle$ [9].

The one-dimensionality is known to induce a gap broadening effect, due to quantum confinement, in H-passivated SiNWs [11]. In this paper we explore on theoretical grounds the electronic structure of SiNWs when the lateral surface is left free to reconstruct. Silicon surfaces are among the most studied systems of the latest decades, both theoretically and experimentally, and it is well-known that the reconstruction drastically affects their electronic properties. In Section 3.1 we discuss the geometry of

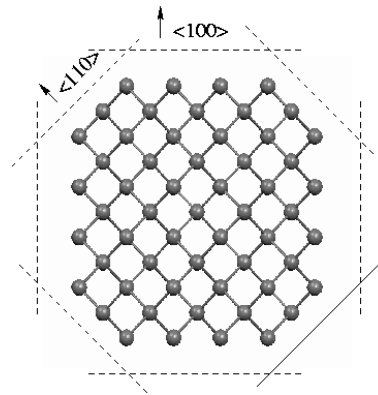


Figure 1. Facet arrangement of a $\langle 110 \rangle$ SiNW as dictated by the Wulff's rule. The formation of $\{110\}$ facets allows a smoother matching between $\{100\}$ facets.

the surface reconstructed SiNWs considered and the implication of the Wulff's rule in the case nanoscale one-dimensional systems. In Section 3.2 we analyse the electronic structure of the most favoured reconstruction and the localisation of the surface states that have been found to form.

2. Computational methods

The calculations presented in this paper have been carried out in the framework of density-functional theory (DFT). We have used both a numerical atomic orbital [12] and a plane-wave [14] basis set. We have used a double-polarised basis set [12] with pseudopotentials of the Troullier-Martins [13] type and a plane-wave energy cutoff of 20 Ry [14] with ultrasoft pseudopotentials [15]. In both cases the exchange-correlation energy was calculated according to the Generalised Gradient Approximation [16]. The wires that we have studied have a diameter of 1.5 nm and a number of atoms ranging from 57 to 171, depending on the supercell size and on the adopted shape of the unrelaxed wire section. The Brillouin zone has been sampled according to the Monkhorst-Pack [17] scheme with a converged grid of $1 \times 1 \times 4$, $1 \times 1 \times 6$ or $1 \times 1 \times 12$ k-points, depending on the supercell size.

3. Results and discussion

3.1. Structural relaxations: checking the Wulff's rule at the nanoscale

Convincing experimental evidence shows that SiNWs are constructed around a crystalline bulk core [8, 18]. The shape of the section of such a structure will depend on the way in which the involved vicinal surfaces match and on how abrupt is the transition from one to the other. The case of SiNWs grown along the $\langle 100 \rangle$ direction is of especial interest, because it determines a rather conflictive situation at the edges where two $\{100\}$ surfaces meet with a 90° angle [see Figure 1 and 2(c)]. In such conditions, it is known

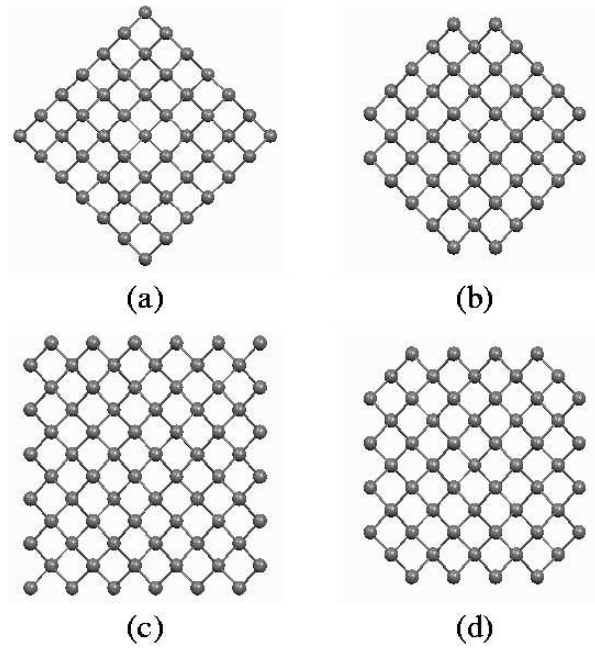


Figure 2. Unrelaxed section of the SiNWs considered.

from Wulff's theorem [19] that the formation of a facet is to be expected, because it would partly release the stress accumulated at the edge. An example of faceting of a $\langle 110 \rangle$ SiNW [20, 21] is shown in Figure 1. As can be seen, the formation of a $\langle 110 \rangle$ facet allows a much smoother transition between the two vicinal $\langle 100 \rangle$ -like surfaces. However, as discussed previously by Zhang and Yakobson [22], in the case of very thin one-dimensional structures such as those that we are treating, the predictions of Wulff's rule should be carefully revised. The size of the $\langle 110 \rangle$ and of the $\langle 100 \rangle$ facets are of the same order of magnitude, thus the surface energy associated to the edges can no longer be neglected, as assumed in Wulff's rule. For these reasons, the first part of this work has consisted in identifying the favoured faceting arrangement of $\langle 110 \rangle$ SiNW of nanometric thickness, thus verifying the validity of Wulff's theorem in these conditions.

We have considered two different square-section wires [Figure 2 (a) and (c)] and two Wulff-faceting arrangements [Figure 2 (b) and (d)]. The square wire of Figure 2 (a) is made of $\langle 110 \rangle$ facets, while the wire in Figure 2 (c) has only $\langle 100 \rangle$ facets. The wires of Figure 2 (b) and (d) have been obtained from those of Figure 2 (a) and (c), respectively, smoothing the corners according to Wulff's rule prescription. The way in which the tension at the edges is released and the way in which the different Si surface reconstructions ($\langle 100 \rangle$ and $\langle 110 \rangle$ facets) compete among them will determine their minimum energy structure. Therefore, given the starting configurations of Figure 2, very different minimum energy structures are expected.

The results of the relaxations are shown in the section-view of Figure 3. As can be seen, all but one of the wires maintain a high degree of in-plane symmetry. As expected, in the SiNW of Figure 3 (a) $\langle 110 \rangle$ facets are dominant. The same relaxation pattern is

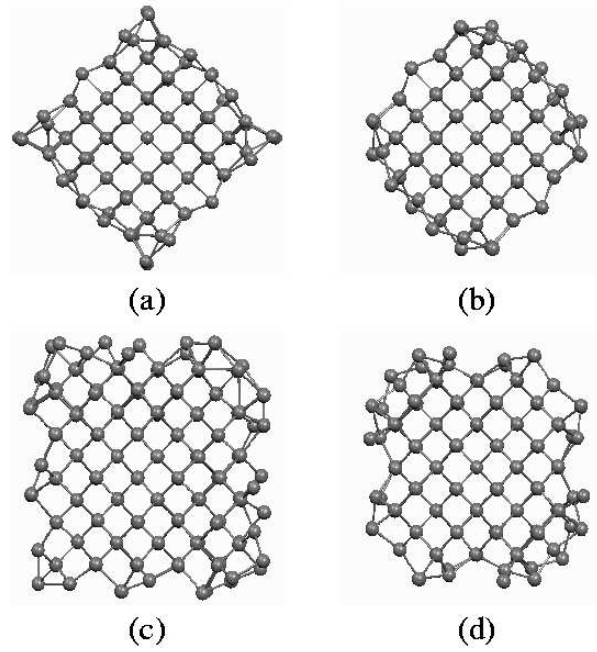


Figure 3. Relaxed section of the SiNWs considered.

followed by the wire of Figure 3 (b), with the only notable exception of the missing corner atoms, whose removal allows a smoother match between the vicinal (110)-like surfaces. In accordance to the prediction of Wulff's rule, the SiNW of Figure 3 (b) turned out to be more stable than that of Figure 2 (a) (the difference amounting to ~ 33 meV/atom).

In the relaxation of the SiNWs of Figure 3 (c) and (d) f100g facets prevail. It is interesting to note that in this case the effects of a Wulff-like profile are more evident than in the former case. Here an actual edge-faceting develops, mediating the transition between the vicinal (100)-like surfaces by f110g facets [see Figure 3 (d)]. On the other hand, when the edges between the f100g facets are not smoothed, the wire favours a symmetry breaking, ending up with the butterfly-shaped section of Figure 3 (c). Interestingly enough, the butterfly wire of Figure 3 (c) has turned out to be slightly more stable than the wire of Figure 3 (d), thus confirming that at such small diameters the validity of Wulff's rule should be carefully checked.

Regarding the influence of facet orientation, we have found that wires dominated by f100g facets [Figure 3 (c) and (d)] are more stable than those where f110g facets prevail [Figure 3 (a) and (b)]. The cohesive energies are summarised in Table 1. For these reasons, the candidate structures for SiNWs grown along the f100g direction appear to be those in Figure 3 (c) and (d), favouring the formation of f100g over f110g facets.

We have found that for the SiNW of Figure 3 (d) two different reconstructions of the f100g facets are possible [21]. Like in the case of the infinite Si(100) surface, the reconstruction consists in the formation of a sequence of buckling dimers. What differs between the two competing geometries that we have obtained is the pattern followed by the Si dimers. In one case they determine a trough in the middle of the facet, while

Dominant facets	Section shape	Cohesive energy (eV/atom)
h110i	square	3.886
h110i	Wul	3.919
h100i	square	4.006
h100i	Wul	3.989

Table 1. Cohesive energies per atoms of the SiNW type illustrated in Fig. 3. The SiNWs where f100g facets prevail are approximately 0.1 eV/atom more stable.

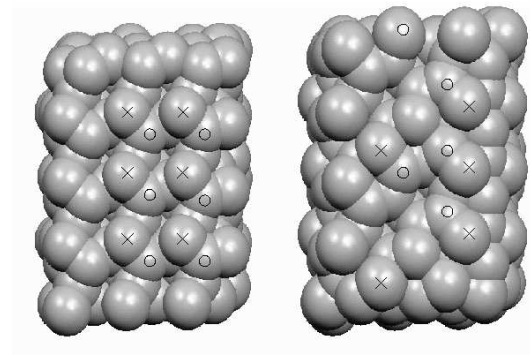


Figure 4. Minimum energy geometries for the facets of h100i butterfly-like SiNW of Figure 3(d).

in the other one every two dimers on one of the two sides is flipped with respect to the symmetric behaviour of the trough reconstruction. The relaxed geometry of the facets of the butterfly wire is shown in Figure 4. The symmetry breaking is reflected in the relaxation and the f100g facets follows two different relaxation patterns. One of them – Figure 4(a) – is rather symmetric, with all the dimers of one side flipped; the facet of Figure 4(b) presents a regular sequence of buckled dimers only in one of the two sides, while in the other one every two dimers is missing.

3.2. Electronic structure

Nanowires – and SiNWs in particular – are expected to play an important role in future molecular electronics applications. Therefore, a thorough understanding of their conductive properties is required. In this section we discuss our results of the electronic structure of the butterfly wire [Figure 3(c)], as well as of the two different reconstructions that we have found for the Wul-like SiNW [Figure 3(d)].

In Figure 5(a) and (b) the band structure diagrams corresponding to the two competing geometries for the Wul-like wire are displayed. It is somehow surprising to discover that they are rather different: while the trough reconstruction is strongly metallic, with four bands crossing the Fermi level, the flipped dimer geometry is only semimetallic, with one band approaching the Fermi energy with a zero derivative at the zone boundary. This is quite striking, at first sight, because the differences between the

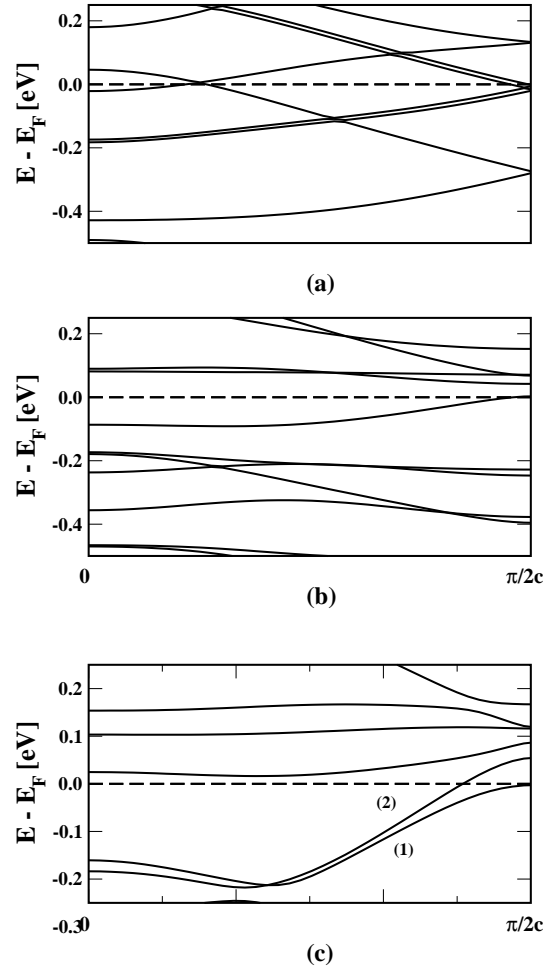


Figure 5. Band structure diagrams of (a) the trough and (b) the dimer-rippled reconstruction of the SiNW with a Wulff-like section; (c) the butterfly-like SiNW.

two reconstructions do not seem to be so relevant. However, when considered in more detail, one notices the pivotal role that the rippled dimer has in breaking the surface Bloch state that would otherwise form. On the contrary, the surface state forms in the trough reconstruction where all the Si dimers follow the same buckling pattern.

The band structure of the butterfly wire is shown in Figure 5(c). Also in this case the reconstruction results in a metallisation of the wire surface, with one band crossing the Fermi level and a semimetallic band tangent to it at the zone boundary. The formation of these metallic and semimetallic states is directly induced by the reconstruction of the surface dimers. Therefore, they are expected to be localised at the wire's outer layers. The dimerisation leads to a dangling bond that hybridises with the other dimers' dangling bonds along the nanowire in a surface π -bond. The surface nature of the semimetallic and metallic states of Figure 5(c) is evident in Figure 6 where we have plotted the corresponding wave functions. As can be seen, the metallic and semimetallic state are localised, at opposite sides, along one of the $h110$ diagonal. A similar surface localisation, though more symmetric, following the pattern of the

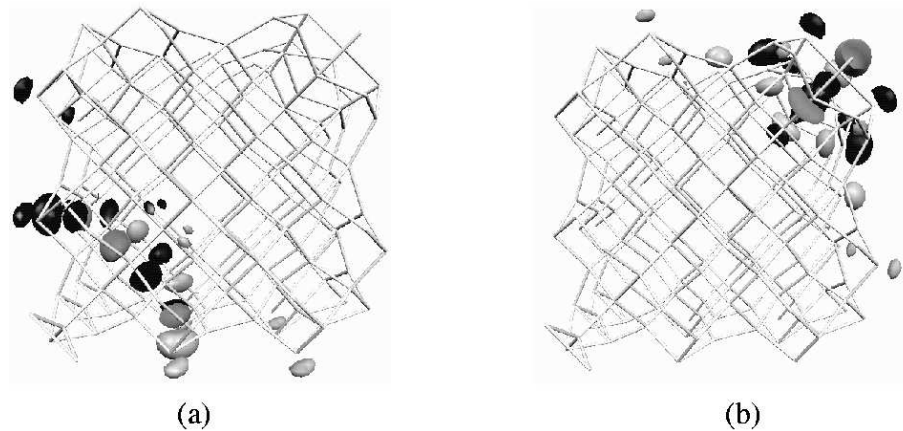


Figure 6. Wave function of (a) the semimetallic and (b) metallic state, respectively labelled as (1) and (2) in Figure 5(c).

overall relaxed geometry, is observed for the Wul-like SiNW of Figure 3(d) (not shown here; see Reference [21]). Therefore, conduction in surface-reconstructed SiNWs will be almost entirely sustained by the outer layers of the wire, with a negligible penetration inside the wire's core. These results, i.e. metallic or semimetallic nature and surface character of the conduction channels, concern all of the h100i wire types that are likely to be obtained. As we have discussed in Section 3.1 (see also Table 1), the difference of cohesive energies among the favoured wire geometries [the wire of Figure 3(c) and the two reconstructions of Figure 3(d)] are very small and the selective growth of one or another wire seems a difficult task.

4. Conclusions

We have shown that in absence of a proper passivation, the lateral surface of SiNWs strongly reconstructs, forming series of buckled dimers with a pattern similar to Si(100) surfaces. Depending on the reconstruction, surface states that cross the Fermi level can form, leading to metallic or semimetallic SiNWs. Under such circumstances, doping is no longer needed to have highly conducting nanowires. The possibility of tailoring SiNWs that are conducting without the need of doping is particularly relevant in very thin wires where typical doping concentrations require a precision in the fraction of impurities per atom extremely difficult to control.

Available experiments have not thoroughly explored the possibility of surface reconstruction or nanowire conductance without doping. However, these results show a promising venue of experimental and theoretical research of pure SiNWs.

R.R. acknowledges the financial support of the Generalitat de Catalunya through a Nanotec fellowship and thanks N. Bedoya for the help in running some calculations. N.L. thanks ACI jeunes chercheurs. Computational resources at the Centre Informatique

National de l'Enseignement Supérieur and the Centre de Calcul Midi-Pyrénées are gratefully acknowledged.

- [1] Appell D 2002 Nature 419 553
- [2] Morales A M and Lieber C M 1998 Science 279 208
- [3] Lieber C M 2002 Nano Lett. 2 81
- [4] Zhou X T, Hu J Q, Li C P, Ma D D D, Lee C S and Lee S T 2003 Chem. Phys. Lett. 369 220
- [5] Cui Y, Wei Q, Park H and Lieber C M 2001 Science 293 1289
- [6] Hahn J and Lieber C M 2004 Nano Lett. 4 51
- [7] Holmes J D, Johnston K P, Doty R C and Korgel B A 2000 Science 287 1471
- [8] Ma D D D, Lee C S, Au F C K, Tong S Y and Lee S T 2003 Science 299 1874
- [9] Wu Y, Cui Y, Huynh L, Barrelet C J, Bell D C and Lieber C M 2004 Nano Lett. 4 433
- [10] Coleman N R B, O'Sullivan N, Ryan K M, Crowley T A, Morris M A, Spalding T R, Steytler D C and Holmes J D 2001 J. Am. Chem. Soc. 123 7010
- [11] Delley B and Steigmeyer E F 1995 Appl. Phys. Lett. 67 2370
- [12] Soler J M, Artacho E, Gale J D, Garcia A, Junquera J, Ordejón P and Sanchez-Portal D 2002 J. Phys.: Condens. Matter 14 2745; <http://www.uam.es/siesta>
- [13] Troullier N and Martins J L 1991 Phys. Rev. B 43 1993
- [14] Hammer B, Hansen L B and Nørskov J K 1999 Phys. Rev. B 59 7413; <http://www.fysik.dtu.dk/campos/>
- [15] Vanderbilt D 1990 Phys. Rev. B 41 7892
- [16] Perdew J P, Burke K and Ernzerhof M 1996 Phys. Rev. Lett. 77 3865
- [17] Monkhorst H J and Pack J D 1973 Phys. Rev. B 8 5747
- [18] Zhang Y F, Liao L S, Chan W H, Lee S T, Sammynaiken R and Sham T K 2000 Phys. Rev. B 61 8298
- [19] Wul G 1901 Zeitschrift für Kristallographie 34 449
- [20] Ismail-Beigi S and Arias T 1998 Phys. Rev. B 57 11923
- [21] Rurali R and Lorente N, in preparation
- [22] Zhao Y and Yakobson B I 2003 Phys. Rev. Lett. 91 035501